

## Efficient Collaborative Spectrum Sensing with Low Sample Rate

L. C. Jiao · Jianrui Chen · Jianshe Wu ·  
Xiaodong Wang · Shuang Zhang

Published online: 23 November 2011  
© Springer Science+Business Media, LLC. 2011

**Abstract** In this paper, collaborate spectrum sensing with incomplete information is considered, which fully exploits the sparsity of active radios. In the traditional collaborate spectrum sensing, the fusion center is applied to determine the locations of idle channels and a lot of sensing information is required to make decision. Too much information is the bottleneck of the collaborative spectrum sensing applications. Here, two novel efficient algorithms based on matching pursuit are presented. Fusion center is also adopted, but the proposed methods can greatly reduce the quantity of necessary sensing information and obtain better detection performance. Simulations have shown that one has much faster sensing speed and the other obtains better detection accuracy. For 20% primary users are active, the detection probability based on the first algorithm can reach 100% only requiring 64% measurements of the traditional collaborative spectrum sensing.

**Keywords** Cognitive radio · Collaborate spectrum sensing · Matching pursuit · Compressive sensing · Sparse model

---

L. C. Jiao · J. Chen (✉) · J. Wu · X. Wang · S. Zhang  
Key Laboratory of Intelligent Perception and Image Understanding of Ministry of Education of China,  
Xidian University, Xi'an, People's Republic of China  
e-mail: jianrui\_chen@sina.com

L. C. Jiao  
e-mail: jlcxidian@163.com

J. Wu  
e-mail: jshwu@mail.xidian.edu.cn

X. Wang  
e-mail: xdwang@mail.xidian.edu.cn

S. Zhang  
e-mail: szhang@mail.xidian.edu.cn

## 1 Introduction

The Federal Communications Commission (FCC) has been considering admitting the cognitive radio (CR) users to access the under-utilized licensed bands on an opportunistic basis with the aid of cognitive radio technology. Spectrum sensing and spectrum management are the key problems in cognitive networks.

In overlay cognitive radio networks, CR users have to frequently perform spectrum sensing before they access the spectrum band. Spectrum sensing can be carried out either individually or cooperatively. In the distributed case, e.g. [1], CR users transmit their information using local common channels in the distributed approach. In the centralized case, a central controller is required, e.g. fusion center, but a lot of sensing information transmission is required. Due to various constraints, collaborations among CR users are important to share the complete spectrum information. It has been shown that, the probability of detecting the primary radio (PR) can be improved through collaboration among CR users [2–4]. During the information is transmitted, due to path loss, channel fading, and/or shadowing effects, the data received in the fusion center is highly damaged. Therefore, the challenge is how to obtain exact channel states from incomplete measurements. Recent studies by the Federal Communications Commission's (FCC) Spectrum Policy Task Force have reported vast temporal and geographic variations in the usage of allocated spectrum with utilization ranging from 15 to 85% [5]. In particular, the spectrum utilization efficiency is shown to be as low as 5% in Singapore [6]. Some research work based on this sparsity of occupied channels have been done. In [7, 8], the authors formulated the collaborative sensing problem as a matrix completion problem and a joint-sparsity problem, which significantly reduced the amount of sensing and transmission workload of cognitive radios for wide range spectrum sensing. The methods in [7, 8] are only suitable to the minor active PRs in the network, but the percentage of active PRs is not limited to 1–3% most of the time.

In this paper, we present two greedy algorithms for spectrum sensing without matrix completion but they can successfully detect active PRs when there are 20% or more PRs. Even our proposed methods are collaborative, the required information is very little. The main idea of greedy algorithm is to iteratively refine a sparse solution by successively identifying one or more components that yield the greatest improvement in quality [9]. Matching Pursuit (MP) and orthogonal matching pursuit are the prior methods for sparse approximation and the related references for this method are [9–12]. Different from the cited references, we consider the jointly sparse matrix recovery problem and further propose two related matrix matching pursuit algorithms.

The spectrum sensing algorithms presented in this paper are Matrix Matching Pursuit (MMP) and Revised Matrix Matching Pursuit (RMMP). Comparing with the methods in [7, 8], the advantages of MMP and RMMP are: (i) higher detection probability with lower sample rate. MMP can obtain 100% detection probability only at the sample rate 0.48 when 10 active among 500 PRs, besides, for 110 active PRs in the network the detection probability can obtain 99.9% at 0.72 sample rate. (ii) lower false alarm probability. The probability of false alarm based on MMP will smaller than  $10^{-4}$  rapidly for all the cases at sample rate is 0.32. (iii) More active PRs. MMP and RMMP also can successfully apply to the case that the spectrum utilization rate is about 20%, which is much more than that of [7, 8]. (iv) Faster sensing time. Without matrix completion and multiple constrained optimization subproblems, MMP and RMMP have faster sensing time. For 110 active PRs existing in the network, MMP in noiseless Rayleigh fading channel model only costs 1.3188 s. The main difference between MMP and RMMP is: MMP is faster than RMMP but RMMP obtains higher detection performance than MMP.

The rest of this paper is organized as follows. The cognitive network model is presented in Sect. 2 and collaborative spectrum sensing is formulated as a minimizing model. In Sect. 3, we present two algorithms *MMP*, *RMMP* and corresponding complexity analysis, respectively. The simulation results are given in Sect. 4 and the conclusions are drawn in Sect. 5.

## 2 Network Model

A cognitive radio environment is considered with  $n$  channels and  $m$  CR users distributed around the channels. In this network surrounding, each channel is occupied by a PR or not occupied. The main objective is to determine which channel is occupied from the sensing data of CR users. Assume that there are  $s$  occupied channels in  $n$  total channels, here  $s < n$ .

Similar to [7, 8], each CR user takes measurements of multiple channels (not all the channels) using equipped frequency selective filters, and then those measurements are sent to the fusion center. Due to energy reservation and the hardware limitation, each CR user might only collect a random (at most  $p$ ) number of reports to the fusion center, which is denoted by a  $p \times n$  filter coefficient matrix  $F$ . The states of all the channels are represented as an  $n \times n$  diagonal matrix  $R$ , where the diagonal entries are 0 for unoccupied channels and 1 for occupied channels. According to the above assumption, there are  $s$  nonzero elements in  $diag(R)$ . Besides, an  $m \times n$  channel gain matrix  $G$  is given by

$$G_{i,j} = P_j(d_{i,j})^{-\alpha/2}|h_{i,j}|, \tag{1}$$

here  $d_{i,j}$  is the distance from the primary transmitter using the  $j$ -th channel to the  $i$ -th CR user,  $\alpha$  is the propagation loss factor,  $P_j$  is the  $j$ -th primary user's transmitted power, and  $h_{i,j}$  is the channel fading. Here, we consider the channel fading is  $h_{i,j} = 1, \forall i, j$  for AWGN(Additive White Gaussian Noise),  $|h_{i,j}|$  follows independent Rayleigh distribution for Rayleigh channel and  $|h_{i,j}|$  follows log-normal distribution for shadowing fading channel [8, 13]. Noise is inevitable in the transmission. So, we consider that the measurement reports sent to the fusion center is corrupted by additive white Gaussian noise  $N_{p \times m}$  and the measurement matrix can be written as the following  $p \times m$  matrix

$$M_{p \times m} = F_{p \times n}R_{n \times n}(G_{m \times n})^T + N_{p \times m}. \tag{2}$$

Generally,  $M$  is incomplete because of transmission failure. Therefore, the received data  $M^E$  is given by:

$$M_{i,j}^E = \begin{cases} M_{i,j}, & (i, j) \in E, \\ 0, & otherwise. \end{cases}$$

Here  $E$  is the indexes set of the locations generated from  $M$  randomly, which denotes the successful received locations in  $M$ . The entries about transmission failure in  $M$  are set to zero. Spectrum sensing problem is to determine the locations of non-zero diagonal elements in  $R$ . If denote  $X = RG^T$ , the problem is equivalent to find the locations of non-zero rows in  $X$ .

Based on the above analysis, we can recover  $X$  from the received  $M^E$ , filter coefficient matrix  $F$  and further determine the locations of active PRs. The model is given by:

$$\begin{aligned} & \min_X \|X\|_0 \\ & s.t. \|FX - M^E\|_F \leq \sigma, \end{aligned} \tag{3}$$

Here vector  $\mathcal{X} \doteq (\|X_{1,\cdot}\|_2, \dots, \|X_{n,\cdot}\|_2)$ ,  $X_{i,\cdot}$  denotes the  $i$ -th row of  $X$  and  $\sigma$  is the estimated noise level.  $\|\cdot\|_0$  represents the number of the non-zero components in the vector. There is some researches on the similar model in the signal processing [14, 15]. Recently, multiple measurement vector problem attracts much interest in sparse representation [16, 17]. But we consider the fact the measurements are lost in the transmission and a lot of entries are set to zero. Here matching pursuit is adopted and modified for our special application in spectrum sensing. It is easy to see that there are only  $s$  rows are nonzero vectors in  $X$  according to  $s$  active PRs in the network. Due to the sparsity of  $X$  and the specialty of spectrum sensing, it is only required to determine the locations of non-zero rows in  $X$ .

It is easy to see that:

$$M = F_{\cdot,1}X_{1,\cdot} + F_{\cdot,2}X_{2,\cdot} + \dots + F_{\cdot,n}X_{n,\cdot} \tag{4}$$

$M$  is the linear combination of  $X_{i,\cdot}$ ,  $i = 1, \dots, n$  and  $F_{\cdot,i}$  is the  $i$ -th column of  $F$ . Due to the utilization rate of spectrum, only  $s$  entries are not zero in  $\mathcal{X}$  in noiseless case. If the energy of  $\hat{X}_{i,\cdot} = F_{\cdot,i}^T M$  is large, it can be concluded that the  $i$ -th row of  $X$  is non-zero with high probability.

Matching pursuit requires the maximum iteration, which can be obtained from the following two methods. Firstly, the possible number of active PR from the history is estimated and denoted as  $w$ . Secondly, the similar result is selected from Ref.[16]:  $iter_{max} = (Spark(F) - 1 + Rank(M))/2$ . Here  $Spark(F)$  is the smallest possible integer such that there exists  $Spark(F)$  columns of matrix  $F$  that are linearly dependent.

### 3 Main Methods for Spectrum Sensing

#### 3.1 Matrix Matching Pursuit

Similar to the vector recovery problem based on matching pursuit, the first algorithm for matrix recovery (termed as Matrix Matching Pursuit) is proposed. Now, look at the  $k$ -th iteration step.

1. Forming a proxy  
 Firstly, we find the projection of  $R^k (R^0 = M^E)$  on each column of  $F$  (i.e.  $\hat{X}_{i,\cdot} = F_{\cdot,i}^T R^k$ ) and calculate each energy of the projection (i.e. 2-norm of  $\hat{X}_{i,\cdot}$ ). Let  $\hat{X}_{i,\cdot}$  be the proxy of  $X_{i,\cdot}$ .
2. Selecting the interested index  
 The index  $i_{max}$  maximizing the above energy is selected. This index indicates the corresponding row in  $X$  is non-zero with high probability.
3. Updating the residual error  
 The new residual error is updated as:  $R^k = R^{k-1} - F_{\cdot,i_{max}} \hat{X}_{i_{max},\cdot}$ . Only the remainder residual error is considered in next iteration.
4. Combining the set of active PRs  
 If  $i_{max}$  is not in the selected set  $I_{busy}^{k-1}$ , update  $I_{busy}^k = I_{busy}^{k-1} \cup i_{max}$ ; otherwise,  $I_{busy}^k = I_{busy}^{k-1}$ . Note that it is possible that the selected index is same in the different iteration step.

The algorithm flow based on  $MMP$  is given as follows.

**Algorithm 1:** The dynamic spectrum sensing based on *MMP*.

- 
- Step 0:** Initialize.  $R^0 = M^E, F, I_{busy}^0 = \emptyset$ .
  - Step 1:**  $\hat{X}_{i,\cdot}^k = F_{:,i}^T R^k$ .
  - Step 2:**  $i_{max} = \operatorname{argmax}_i \|\hat{X}_{i,\cdot}^k\|_2$ .
  - Step 3:**  $R^k = R^{k-1} - F_{:,i_{max}} \hat{X}_{i_{max},\cdot}^k$ .
  - Step 4:**  $I_{busy}^k = I_{busy}^{k-1} \cup i_{max}$ . Iterate from Step 1 until stopping criteria are satisfied.
- 

The termination for Algorithm 1 has the following two possibilities:

- Stop the algorithm after a fixed number  $k$  of iterations, i.e., when  $k = \operatorname{iter}_{max}$ . In order to avoid the interference to the PR, let  $\operatorname{iter}_{max} = w + 5$  or  $\operatorname{iter}_{max} = (\operatorname{Spark}(F) - 1 + \operatorname{Rank}(M))/2$ .
- Iterate until  $\|\hat{X}_{i_{max},\cdot}^k\|_2$  declines to a level  $tol$ , which can ensure high accuracy before termination. And in simulations  $tol$  is set to  $1e - 3$ .

### 3.2 Revised Matrix Matching Pursuit

The higher recovery accuracy of  $X$  should be assured in each iteration step to obtain higher detection probability. So, we propose the second algorithm based on revised matrix matching pursuit (termed as *RMMP*) with the minimal residual error assurance in each step. *RMMP* differs from *MMP* mainly in the rule of index selection in Step 2. *RMMP* depends on the minimum index about  $\|R^{k-1} - F_{:,i} \hat{X}_{i,\cdot}^k\|_F$  while *MMP* depends on the maximum index about  $\|\hat{X}_{i,\cdot}^k\|_2$ . It is easy to see that *RMMP* can assure higher accuracy of recovered  $\hat{X}^k$  in each step, so, it can obtain higher detection probability than *MMP*.

**Algorithm 2:** The dynamic spectrum sensing based on *RMMP*.

- 
- Step 0:** Initialize.  $R^0 = M^E, F, I_{busy}^0 = \emptyset$ .
  - Step 1:**  $\hat{X}_{i,\cdot}^k = F_{:,i}^T R^k$ .
  - Step 2:**  $i_{max} = \operatorname{argmin}_i \|R^{k-1} - F_{:,i} \hat{X}_{i,\cdot}^k\|_F$ .
  - Step 3:**  $R^k = R^{k-1} - F_{:,i_{max}} \hat{X}_{i_{max},\cdot}^k$ .
  - Step 4:**  $I_{busy}^k = I_{busy}^{k-1} \cup i_{max}$ . Iterate from Step 1 until stopping criteria are satisfied.
- 

The termination for Algorithm 2 has the similar two possibilities:

- Stop the algorithm after a fixed number  $k$  of iterations, i.e., when  $k = \operatorname{iter}_{max}$ . Similarly, let  $\operatorname{iter}_{max} = w + 5$  or  $\operatorname{iter}_{max} = (\operatorname{Spark}(F) - 1 + \operatorname{Rank}(M))/2$ .
- Iterate until the F-norm of the residual error declines to a level  $tol$ . That is  $\|R^k\|_F < tol$ . And  $tol$  is  $1e - 3$  in simulations.

Remark: If  $\operatorname{iter}_{max} = w + 5$  is adopted to terminate the algorithms, the prior about the possible number of active PRs in the network is required. This prior can obtain better higher detection probability and lower false alarm probability. If the prior is unknown in advance,

**Table 1** The complexity of *MMP*, *RMMP* and Algorithm 1 in Ref. [8]

	Step 1	Step 2	Step 3	Total complexity
<i>MMP</i>	$O(pmn)$	$O(mn)$	$O(pm)$	$O(pmn)$
<i>RMMP</i>	$O(pmn)$	$O(pmn)$	–	$O(pmn)$
Ref. [8]				$O(mn^3)$

$iter_{max} = (Spark(F) - 1 + Rank(M))/2$  is selected, which requires the information about *F* and *M*.

### 3.3 Complexity Comparison

Computational complexity of *MMP* and *RMMP* are computed and compared in Table 1, which are mainly about multiply operation in each iteration. Here, parallel computing is not considered. The complexity of *MMP* and *RMMP* are similar, but *MMP* is faster than *RMMP* in simulations. This is mainly because the main computation in *RMMP* is matrix norm and that of *MMP* is vector norm. In Ref. [8], it has been shown that matrix completion recovery is slower than jointly sparsity recovery. Therefore, the total complexity of only Algorithm 1 (jointly sparsity recovery) in Ref. [8] is listed in Table 1. Multiple constrained optimization subproblems are the main procedure of the Ref. [8] and they need a lot of computational time. The complexity of a constrained optimization algorithm ‘logprog’ is about  $O(n^3)$  given in Ref. [18]. The number of such constrained optimization problems is the number of the columns in *X* (i.e. *m*). Then, the total complexity of Algorithm 1 in Ref. [8] is about  $O(mn^3)$ . It is obvious that our proposed methods are faster than Ref. [8] due to the sample rate is low, i.e.  $p < n$  in general.

## 4 Performance Evaluations

The network model considered here is same as Ref. [8]: primary users are uniformly distributed in a  $1,000 \times 1,000$  m square area and CR users are uniformly distributed in a  $500 \times 500$  meter square area, all centered at the fusion center. The number of the primary users is  $n = 500$  and that of the CR users is  $m = 10$ . Unless noted otherwise, the number of the reports for each CR user is  $p = 400$  and the received entries in the fusion center are randomly selected from *M* uniformly. The sample rate is defined as [7,8]:

$$sr \triangleq \text{sample rate} = \frac{|E|}{m \times n}. \tag{5}$$

Here  $|E|$  is the cardinality of the set *E*. The denominator in (5) is the required information for the traditional spectrum sensing based on the fusion center. Define the received rate from *M* as:

$$\text{rate} = \frac{|E|}{m \times p}. \tag{6}$$

In simulations, *rate* is changed from 0.1 to 1. In order to make our discussion as general as possible, the locations of nonzero rows are selected randomly. Filter coefficient matrix *F* is selected from the Gaussian distribution. In the figures, ‘*r = i*’ represents the number of occupied channels is *i*.

The same concepts are defined as [7]:

$$\begin{aligned}
 PoD \triangleq \text{Probability of Detection} &= \frac{\text{No. Hit}}{\text{No. Hit} + \text{No. Miss}}, \\
 FAR \triangleq \text{False Alarm Rate} &= \frac{\text{No. false alarm}}{\text{No. false alarm} + \text{No. Hit}}, \\
 MDR \triangleq \text{Miss Detection Rate} &= \frac{\text{No. Miss}}{\text{No. Miss} + \text{No. Correct}},
 \end{aligned}
 \tag{7}$$

where No. Hit is the number of successful detection of the appearance of active PRs, No. Miss is the number of miss detection of the appearance of active PRs, No. false alarm is the number of the non-active PRs detected as active and No. Correct is the number of correct reports of no appearance of PRs.

Besides, the probability of false alarm is also adopted given as

$$PoF \triangleq \text{Probability of False alarm} = \frac{\text{No. err\_occupied}}{n - \text{No. Hit} - \text{No. Miss}},
 \tag{8}$$

here *No.err\_occupied* is the number of the non-active primary users detected as active. In each iteration step, *MMP* and *RMMP* only select the best index according to the selection criterion and here we select  $iter_{max} = s + 5$  to test the performance of *MMP* and *RMMP*. In simulations, the number of occupied channels  $s = 10, 50, 110, 130, 190, 250$ , respectively out of the total channels  $n = 500$ . If the possible number of active radios is unknown, we can select  $iter_{max} = (Spark(F) - 1 + Rank(M))/2$  according to Ref. [16]. Besides, a possible active radio is selected in each iteration and the range of active radios is [0,500], so we can select  $iter_{max} = 500$ , too. The two selection can obtain similar detection probability but need lots of running time due to large iterations.

$h_{i,j}$  in (1) is given as: in AWGN channel model,  $h_{i,j} = 1, \forall i, j$ ; in Rayleigh fading channel model, Joke’s model of Rayleigh fading is adopted and the number of sinusoids is 8, the number of uncorrelated rayleigh fading functions is 6; in log-normal shadowing fading channel,  $h_{i,j}$  is generated by *lognrnd*(0, 1/4) random log-normal distribution. The propagation loss factor  $\alpha = 1.5$ .

#### 4.1 Detection Performance Analysis

In spectrum sensing, we hope to obtain the following result: higher PoD and lower PoF, MDR in a relatively short time. Figures 1, 2, and 3 show the detection performance based on *MMP* in  $SNR = 15$  dB Rayleigh fading channel, log-normal shadow fading channel and AWGN channel, respectively. It can be observed that these three channel model show almost the same performance in PoD, PoF and MDR. Besides, it is easy to find that the PoD is decreasing with the number of occupied channels, while PoF is increasing with the number of occupied channels at the same sample ratio. The reason is that *MMP* and *RMMP* are based on the compressed sensing theory, which is derived from the sparse representation. The detection performance will be degraded when  $X$  is not sparse.

Figure 4 gives the corresponding PoD and PoF based on *RMMP* in  $SNR = 15$  dB AWGN channel model. The PoD based on *MMP* is 100% for all cases when  $sr > 0.64$ . In fact, PoD based on *MMP* and *RMMP* is more than 99.4% for  $r = 10$  when  $sr > 0.4$ . While the same detection performance in Ref. [8] requires the sample rate is 0.62 even in noiseless case. Besides, the detection performance of *RMMP* is slightly better than that of *MMP* for minor active PRs existing in the network. For  $r = 10$ , the PoD of *RMMP* is

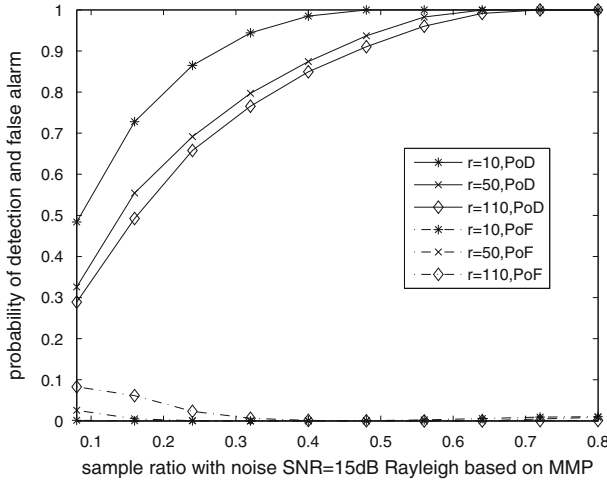


**Fig. 1** PoD and PoF based on *MMP* versus sampling rate in Rayleigh fading channel model with  $SNR = 15$  dB. The above curves represent the corresponding PoD and the below curves for PoF

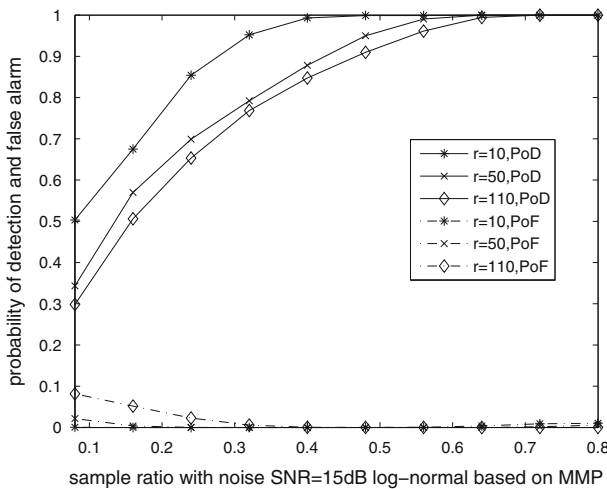


**Fig. 2** PoD and PoF based on *MMP* versus sampling rate in log-normal shadow fading channel model with  $SNR = 15$  dB. The above curves represent the corresponding PoD and the below curves for PoF

higher than 99.6% since the sample rate is 0.24, while that of *MMP* is higher than 99.5% after the sample rate is 0.4.

We compare the overall performance  $r = 1, 5, 11, 50, 110$  based on *MMP*, *RMMP* and Algorithm 1 in Ref. [8] in Table 2, here  $sr = 50\%$ , ‘N’ means noise  $SNR = 15$  dB in Rayleigh fading channel and ‘L’ means noiseless in AWGN fading channel. It can be seen that *MMP*, *RMMP* can obtain higher PoD and lower MDR than Algorithm 1 in Ref. [8]. But FAR is higher, which is due to the fact that the maximum iterations is set larger than the real number of active PRs. *MMP* and *RMMP* can select an interested index in each iteration and larger maximum iterations will result in the unwanted indexes are selected. For more active PRs in the network, e.g.  $r = 11$ , the FAR is lower than Ref. [8].



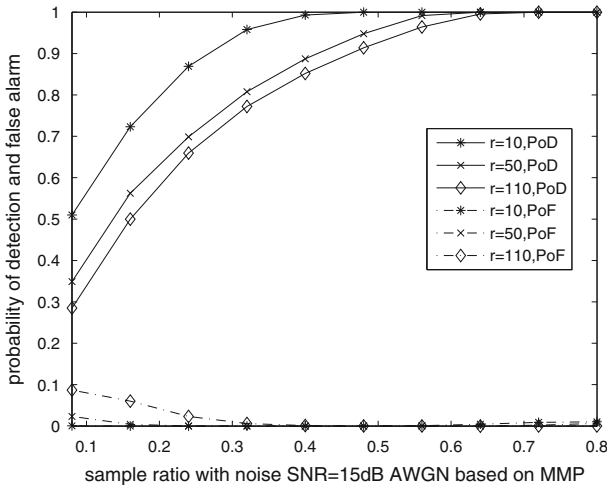


**Fig. 3** PoD and PoF based on *MMP* versus sampling rate in AWGN channel model with  $SNR = 15$  dB. The above curves represent the corresponding PoD and the below curves for PoF

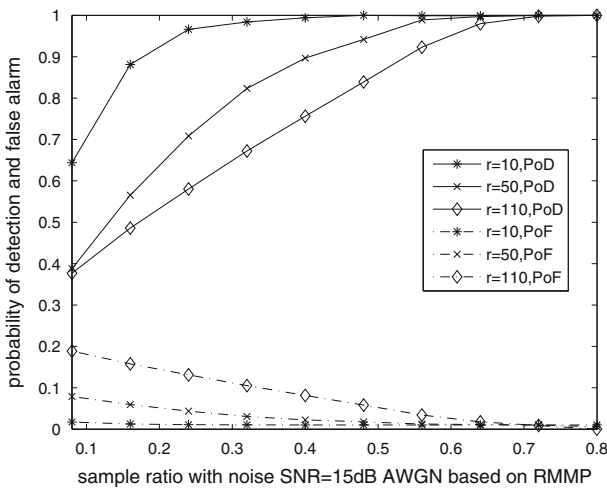


**Fig. 4** PoD and PoF based on *RMMP* versus sampling rate in  $SNR = 15$  dB AWGN channel model. The above curves represent the corresponding PoD and the below curves for PoF

#### 4.2 Impact of Different SNR

The proposed methods can obtain better performance even if there is larger noise. Figure 5 shows the POD and POF with different SNR in Rayleigh channel based on *MMP*,  $sr = 0.56$ . It can be observed that POD and POF obtain satisfactory results after  $SNR = 10$  dB.

#### 4.3 General Case

The proposed methods are based on the sparsity of active PRs' locations. In fact, the utilization rate of spectrum bands may be higher than the previous discussion. This is due to (i)

**Table 2** The performance of *MMP*, *RMMP* and Algorithm 1 in Ref. [8]

		r = 1 (N)	r = 5 (N)	r = 11 (N)	r = 50 (L)	r = 110 (L)
Ref. [8]	PoD	1	<0.7	0.4	0.2880	0.1227
	FAR	<0.25	<0.4	<0.25	0.0036	0.0036
	MDR	0	>0.0025	>0.01	0.0732	0.1983
<i>MMP</i>	PoD	1	1	1	0.9628	0.9278
	FAR	0.8333	0.6207	0.1916	0	0
	MDR	0	0	0	0.0041	0.0199
<i>RMMP</i>	PoD	1	1	1	0.8602	0.7319
	FAR	0.7807	0.2010	0.0366	0.0266	0.0844
	MDR	0	0	0	0.0151	0.0695

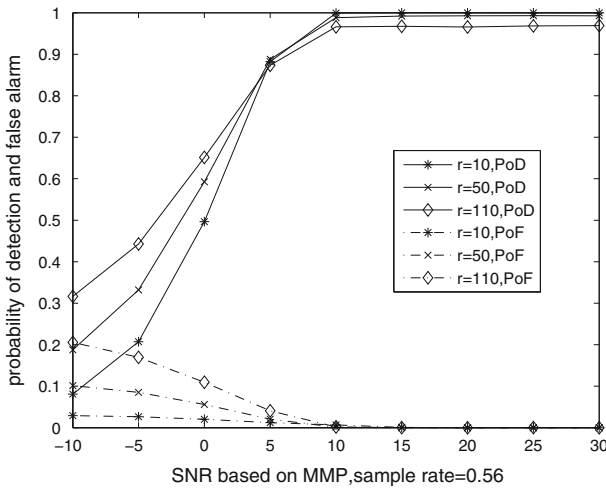


**Fig. 5** PoD and PoF with different SNR, sample rate = 0.56

more PRs are active in the network at some time period; (ii) the other secondary users may access these spectrum in advance and we hope less conflict happens in the network. So, the number of active channels is extended to  $s = 250$ . The following simulations are based on *MMP* in noiseless AWGN channel and given in Fig. 6. It can be observed that even for half of PRs are active, detection probability based on *MMP* is higher than 91% when sample rate is 0.64. Detection performance varies slightly with the number of active PRs.

#### 4.4 Running Time Based on *MMP* and *RMMP*

The running time of *MMP* and *RMMP* are stable for different channel model, i.e. it is generally same for AWGN, Rayleigh fading and log-normal shadowing channel model. So, Fig. 7 only gives the running time based on *RMMP* in Rayleigh channel model and *MMP* in AWGN channel model, respectively. The simulation results are consistent with the complexity analysis in Sect. 3.3. *MMP* is faster than *RMMP* and their running time is almost

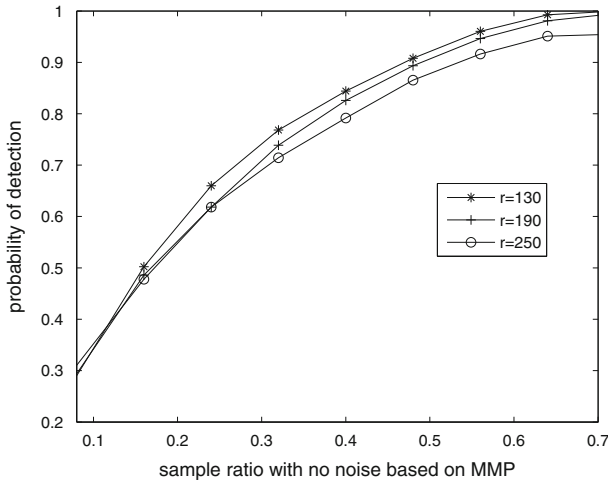


Fig. 6 Detection probability with more active among 500 PRs

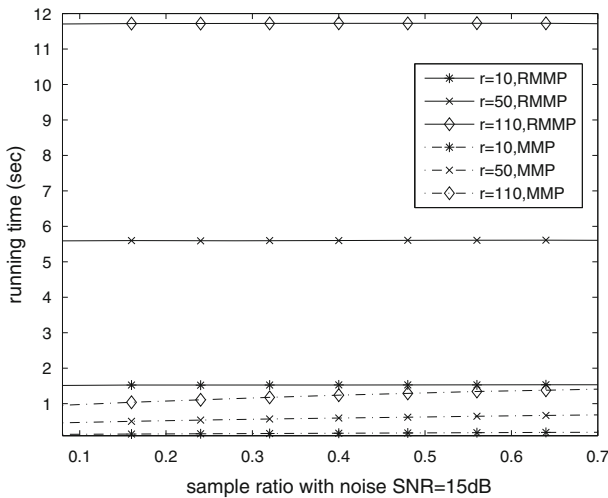


Fig. 7 Running time based on MMP and RMMP

stable with different sample rate. Simulation tests are executed at the 1GB Memory Intel(R) Pentium (R)4CPU, 3.20 GHz.

Table 3 also presents the running time of MMP, RMMP and Algorithm 1 in Ref. [8] in noiseless case. It can be observed that MMP and RMMP are much faster than Algorithm 1 in Ref. [8] no matter how many PRs exist in the network. Even if there are many RRs existing, e.g.  $r = 110$ , MMP is still much faster than Algorithm 1 in Ref. [8]. The main reason is our proposed methods adopt matching pursuit avoiding the multiple constrained optimization subproblems.

**Table 3** The running time of *MMP*, *RMMP* and Algorithm 1 in Ref. [8]

	$r = 10$ , AWGN	$r = 50$ , Log-normal	$r = 110$ , Rayleigh
Ref. [8]	91.5884	89.6791	90.0336
<i>RMMP</i>	0.1969	0.6422	1.3188
<i>MMP</i>	1.5402	5.5942	11.6852

## 5 Conclusions

In this paper, we consider adopting matching pursuit to detect spectrum holes in cognitive network, which not only greatly reduces the quantity of sensing information transmitted but also obtains satisfactory detection performance. Firstly, a simple *MMP* algorithm is proposed for spectrum sensing based on vector matching pursuit. Secondly, we present *RMMP* to obtain higher detection performance, which can obtain better detection probability better than *MMP* when minor PRs existing in the network. For example, when  $r = 190$ , *RMMP* can obtain 44.7% detection probability at the sample rate 0.08, while detection probability based on *MMP* is 29.4%. Note that both *MMP* and *RMMP* can obtain better performance than Ref. [8]. But the percentage of active users is large in some certain time period and the FAR based on our methods is relative high. We hope give more general algorithm in the future.

**Acknowledgments** This research was supported through the Key Scientific and Technological Innovation Special Projects of Shanxi“13115”,(No. 2008ZDKG-37); the National Natural Science Foundation of China (No.61072106, 61072139,61003199); the Fund for Foreign Scholars in University Research and Teaching Programs(the 111 Project)(B07048); the Fundamental Research Funds for the Central Universities: JY10000902001, K50510020001, JY10000902045, JY10000902036; the Open Research Fund Program of Key Lab of Intelligent Perception and Image Understanding of Ministry of Education of China under Grant: IPIU012011003.

## References

1. Li, Z., Yu, F. R., & Huang, M. (2009). *Distributed spectrum sensing in cognitive radio networks*. In *Proceedings of IEEE WCNC09*, Budapest, Hungary.
2. Ghasemi, A., & Sousa, E. S. (2005). Collaborative spectrum sensing for opportunistic access in fading environments. In *IEEE symposium new frontiers in dynamic dpectrum access networks* (pp. 131–136). Baltimore, USA.
3. Visotsky, E., Kuffner, S., & Peterson, R. (2005). On collaborative detection of TV transmissions in support of dynamic spectrum sensing. In *IEEE symposium new frontiers in dynamic spectrum access networks* (pp. 338–356). Baltimore, USA.
4. Zhang, W., & Letaief, K. B. (2008). Cooperative spectrum sensing with transmit and relay diversity in cognitive networks. *IEEE Transactions on Wireless Communications*, 7, 4761–4766.
5. FCC. (2002). Spectrum policy task force report, ET Docket No. 02-155.
6. Islam, M. H., Koh, C. L., Oh, S. W., Qing, X., Lai, Y. Y., Wang, C., et al. (2011). Spectrum survey in Singapore: Occupancy measurements and analysis. In *Proceedings of IEEE CROWNCOM'08, Singapore* (pp. 1–7).
7. Meng, J., Yin, W., Li, H., Houssain, E., & Han, Z. (2010). Collaborative spectrum sensing from sparse observations using matrix completion for cognitive radio networks. In *35th international conference on acoustics, speech, and signal processing (ICASSP)*.
8. Meng, J., Yin, W., Li, H., Houssain, E., & Han, Z. (2011). Collaborative spectrum sensing from sparse observations in cognitive radio networks. *IEEE Journal on Selected Areas in Communications*, 29(2), 327–337.
9. Mallat, S. G., & Zhang, Z. (1993). Matching pursuits with time-frequency dictionaries. *IEEE Transactions on Signal Processing*, 41, 3397–3415.

10. Pati, Y. C., Rezaifar, R., & Krishnaprasad, P. S. (1993). Orthogonal matching pursuit: Recursive function approximation with applications to wavelet decomposition. In *Proceedings of 27th annual asilomar conference on signals, systems and computers*.
11. Davis, G., Mallat, S., & Avellaneda, M. (1997). Adaptive greedy approximation. *Journal of Constructive Approximation*, 13, 57–98.
12. Tropp, J., & Wright, S. (2009). Computational methods for sparse solution of linear inverse problems. *Technical Report No. 2009-01*. California: Institute of Technology.
13. Rappaport, T. S. (2002). *Wireless communications: Principles and practice, 2nd edn*. Englewood Cliffs, NJ: Prentice Hall.
14. Cotter, S. F., Rao, B. D., Egan, K., & Delgado, K. K. (2005). Sparse solutions to linear inverse problems with multiple measurement vectors. *IEEE Transaction on Signal Processing*, 53, 2477–2488.
15. Tropp, J. A., Gilbert, A. C., & Strauss, M. J. (2006). Algorithms for simultaneous sparse approximation. Part. I: Greedy pursuit. *Signal Processing*, 86, 572–588.
16. Chen, J., & Huo, X. M. (2006). Theoretical results on sparse representations of multiple-measurement vectors. *IEEE Transactions on Signal Processing*, 54(12), 4634–4643.
17. Berg, E., & Friedlander, M. P. (2010). Theoretical and empirical results for recovery from multiple measurement. *IEEE Transactions on Information Theory*, 56(5), 2516–2527.
18. Zhang, Y. (1995). Solving large-scale linear programs by interior-point methods under the matlab environment. *Technical Report TR96-01*. Baltimore County, Baltimore, MD: Department of Mathematics and Statistics, University of Maryland.

## Author Biographies



**L. C. Jiao** (SM'89) received the B.S. degree from Shanghai Jiaotong University, Shanghai, China, in 1982, and the M.S. and Ph.D. degrees from Xi'an Jiaotong University, Xi'an, China, in 1984 and 1990, respectively. He currently works as a Distinguished Professor with the School of Electronic Engineering, Xidian University, Xi'an, China. His research interests include signal and image processing, natural computation and intelligent information processing. He is an IEEE senior member, member of IEEE Xi'an Section Executive Committee, and the Chairman of Awards and Recognition Committee, executive committee member of Chinese Association of Artificial Intelligence. He has charged of about 40 important scientific research projects, and published more than 10 monographs and a hundred papers in international journals and conferences.



**Jianrui Chen** was born in Inner Mongolia, China, on March 28, 1979. She received the B.S. degree from the Institute of Mathematical Sciences, Inner Mongolia Normal University, China and the M.S. degree in College of Science, Inner Mongolia University of Technology, China, in 2002 and 2007, respectively. She is currently working toward the Ph.D. degree in Xidian University, Xi'an, China and she is a lecturer in the College of Science at Inner Mongolia University of Technology, China. Her current research interests include cognitive wireless networks, game theory and its applications. She has published several papers in some leading journals, such as *Nonlinear analysis: real world applications*.



**Jianshe Wu** was born in Shaanxi, China, on May 25, 1969. He received the B.S. degree from the Sichuan University, and the M.S. degree and Ph.D. degree from Xidian University. Now, he is an Associate Professor of the Key Laboratory of Intelligent Perception and Image Understanding of Ministry of Education of China. His current research interests include multi-agent systems, game theory and cognitive wireless networks. She has published many papers in some leading journals such as *Physica A*, *Physica D*, *IEEE transaction on circuit and systems*.



**Xiaodong Wang** was born in Heilongjiang province, China, on June, 1975. He received the B.S. degree from Department of Mathematics, Harbin Institute of technology, China, and the M.S. degree from Inner Mongolia University of Technology, China, in 1998 and 2007, respectively. He is currently working toward the Ph.D. degree in Xidian University, Xi'an, China. His current research interests include convex optimization and its applications in compressive sensing and wireless networks.



**Shuang Zhang** was born in Liao Ning, China, on September 22, 1983. She received the B.S. degree from the Institute of Communication Engineering, Liao Ning University, China in 2006. She is currently working toward the Ph.D. degree in Xidian University, Xi'an, China. Her current research interests include multimedia communication and cognitive radio networks.